Modeling Failure in Composite Materials with the Extended Finite Element and Level Set Methods

Matthew J. Pais[1] and Nam-Ho Kim[2]
University of Florida, Gainesville, FL 32611

When modeling crack growth in composite materials, one encounters strong (cracks) and weak (material interface) discontinuities. Traditional finite element methods require the mesh to conform to the material interface and crack surface. In addition, costly remeshing is required as crack growth occurs. In this paper, the extended finite element method (XFEM) coupled with the level set method is presented to model both strong and weak discontinuities. For the material interface, an element-based enrichment function is introduced, which shows more consistent behavior than the node-based enrichment function. The XFEM crack implementation and element-based bi-material implementation are validated using analytical solutions.

Nomenclature

a	=	crack length
a_I, b_I	=	enriched nodal degrees of freedom associated with enrichment functions
$h(\mathrm{x})$	=	Heaviside enrichment function
$H(x)$	=	shifted Heaviside enrichment function
N_I	=	finite element shape functions
r	=	distance from crack tip to a point of interest
r_c	=	radius of fiber
u, v	=	x, y-components of interface velocity
$u^h(x)$	=	XFEM displacement approximation
u_I	=	nodal degree of freedom vector associated with continuous finite element solution
$\vec{V}$	=	velocity field for level set method
x_i, y_i	=	x, y-coordinates of the ith node
x_c, y_c	=	x, y-coordinates of the center of the fiber
$\mathcal{N}$	=	set of all nodes in the mesh
$\mathcal{N}_e$	=	set of all enriched nodes
$\mathcal{N}_\Gamma$	=	set of nodes whose shape function is cut by the crack
$\mathcal{N}_\Lambda$	=	set of nodes whose shape functions are cut by the crack tip
α	=	generic index
Δx, Δy	=	grid density in x, y-directions
$\zeta(x)$	=	level set function representing fiber
θ	=	angle from crack to point of interest in the crack tip coordinate system
θ_c	=	angle of crack growth

[1] Graduate Research Assistant, Department of Mechanical and Aerospace Engineering, PO Box 116250 Department of Mechanical and Aerospace Engineering, University of Florida, Gainesville, FL 32611-6250, and Student Member.
[2] Associate Professor, Department of Mechanical and Aerospace Engineering, PO Box 116250 Department of Mechanical and Aerospace Engineering, University of Florida, Gainesville, FL 32611-6250, and AIAA Member.

λ	=	scaling parameter associated with a crack in a finite plate given as crack length divided by area
$\phi(x)$	=	level set function normal to crack
$\phi_\alpha(x)$	=	linear elastic asymptotic crack tip enrichment function
$\Phi_\alpha(x)$	=	shifted linear elastic asymptotic crack tip enrichment function
$\upsilon(x)$	=	generic enrichment function
$\upsilon_I(x)$	=	generic enrichment function evaluated at node I of an element
$\Upsilon(x)$	=	generic shifted enrichment function
$\psi(x)$	=	level set function tangent to crack
Ω	=	domain of interest

I. Introduction

ACCURATELY modeling discontinuities that are present in materials is a challenging engineering task. Originally the finite element framework was modified to accommodate the discontinuities that are caused by phenomena such as cracks, inclusions and voids. The finite element framework is not well suited for modeling crack growth because the domain of interest is defined by the mesh. At each increment of crack growth, at least the domain surrounding the crack tip must be remeshed such that the updated crack geometry is accurately represented.

The extended finite element method (XFEM) can be used to alleviate many of the inconveniences of using the finite element method (FEM) to model the evolution of a crack. Special enrichment functions are added to the traditional finite element framework through the partition of unity framework. For modeling the strong discontinuity of a cracked body two enrichment functions are used. The Heaviside step function represents the discontinuity away from the crack tip and the linear elastic asymptotic crack tip displacement fields are used to account for discontinuity at the crack tip. The crack is represented independent of the mesh by the enrichment functions which allows for the crack geometry to be updated without a need to create/update a new mesh on the domain. For the case of a material interface, an enrichment function is used which combines distance from the weak discontinuity and the absolute value function.

Since the crack is independent of the mesh it can be challenging to accurately track the growth of the crack as it evolves over time. To this end the level set method is used to represent and update the crack geometry. The level set method is a numerical algorithm which models the evolution of a boundary or interface. The interface of interest is defined to be the zero level set of a function of one higher dimension. Since the level set method was originally used only for tracking closed boundaries, a modified version introduced to represent and track open line segments is used here. The use of the level set method also simplifies the selection of enriched nodes.

Crack growth was modeled using the maximum circumferential stress criterion. This criterion is selected based on its ease of use in being integrated into a computational algorithm. The stress intensity factors needed for this criterion were calculated using the domain form of the J-integral interaction integrals.

The combined use of the extended finite element and level set methods will be used to study crack propagation in composite materials. An emphasis will be made on the crack growth as it approaches the fiber reinforcement within a composite matrix. The goal is to be able to accurately assess if failure occurs as a result of crack penetration into the fiber or debonding between the fiber and matrix.

II. Extended Finite Element Method

The extended finite element method allows discontinuities such as cracks[1-5], inclusions[6] and voids[6,7] to be represented in the finite element domain independent of the mesh[1]. Cracks in two[1-4,8,9] and three[5,8,10,11]-dimensions have been modeled, including those with arbitrary branches[7] and bi-material cracks[12]. Cohesive crack growth[13,14] has also been modeled using the XFEM. While many discontinuous structures have been modeled using XFEM, modeling of composite materials has seen less interest. Hettich[15,16] has shown progress in the modeling of composite materials including debonding[16] and small-scale composite material failure[15].

Arbitrary discontinuities are modeled independent of the finite element mesh by enriching the finite element approximation with additional functions to model the discontinuities. In general the approximation of displacement field in XFEM takes the following form[1]:

$$u^h(\mathbf{x}) = \sum_{I \in \mathcal{N}} N_I(\mathbf{x})\left[\mathbf{u}_I + \underbrace{\upsilon(\mathbf{x})\mathbf{a}_I}_{I \in \mathcal{N}_e}\right] \tag{1}$$

where $N_I(x)$ are the FEM shape functions, u_I are the nodal displacements associated with the continuous part of the approximation, $\upsilon(x)$ is an enrichment function, a_I are additional degrees-of-freedom (DOFs) associated with the discontinuous part of the approximation and $\mathcal{N}_e$ is the set of enriched nodes. It is noted that Eq. (1) does not satisfy the interpolation property; i.e., $u^h(\mathbf{x}_I) \neq u_I$. The actual displacement at a node is a combination of the u_I and a_I. Therefore it is convenient to modify Eq. (1) such that the displacement is of the form[2]:

$$u^h(\mathbf{x}) = \sum_{I \in \mathbb{N}} N_I(\mathbf{x})\left[\mathbf{u}_I + \underbrace{\Upsilon(\mathbf{x})\mathbf{a}_I}_{I \in \mathbb{N}_e}\right] \tag{2}$$

where $\Upsilon(x)$ is given as

$$\Upsilon(x) = \upsilon(x) - \upsilon_I \tag{3}$$

where υ_I is the value of the enrichment function at node I. Thus the enrichment function is shifted such that it is now zero at the nodes. This means that the displacement approximation at node I takes the following form:

$$u^h(x_I) = \sum_J N_J(x_I)u_J = u_I \tag{4}$$

since the enrichment function vanishes at the nodes. Here a general enrichment function is denoted by $\upsilon(x)$ while the corresponding shifted enrichment function such that the enrichment is zero at the nodes is denoted by $\Upsilon(x)$. A description of the various enrichment functions used for modeling composite material behavior follows along with an example of the stiffness matrix calculation in the XFEM.

First the enrichment functions for a crack are considered. The generalized Heaviside step function is used to model the interior of a crack[3]. The Heaviside function h is given by

$$h(\mathbf{x}) = \begin{cases} +1 & \text{Above Crack} \\ -1 & \text{Below Crack} \end{cases}. \tag{5}$$

For those elements that are cut by a crack, the Heaviside step function is multiplied by nodal enriched DOFs to enrich the displacement.

The crack tip is modeled using a crack-tip enrichment function which incorporates the radial and angular behavior of the two-dimensional asymptotic crack-tip displacement field[1]. The crack tip enrichment functions in isotropic elasticity are given by

$$\left[\phi_\alpha(x), \alpha = 1-4\right] = \left[\sqrt{r}\sin\frac{\theta}{2}, \sqrt{r}\cos\frac{\theta}{2}, \sqrt{r}\sin\theta\sin\frac{\theta}{2}, \sqrt{r}\sin\theta\cos\frac{\theta}{2}\right] \tag{6}$$

where r and θ are polar coordinates in the local crack-tip coordinate system. For the element that contains the crack tip, the above functions are multiplied by nodal enriched DOFs to enrich the displacement. When a node is enriched by both of Eqs. (5) and (6), Eq. (6) is used.

For two-dimensional crack modeling the enriched displacement function in XFEM follows the following form:

$$\mathbf{u}^h(\mathbf{x}) = \sum_{I \in \mathcal{N}} N_I(\mathbf{x}) \left[\mathbf{u}_I + \underbrace{H(\mathbf{x})\mathbf{a}_I}_{I \in \mathcal{N}_\Gamma} + \underbrace{\sum_{\alpha=1}^4 \Phi_\alpha(\mathbf{x})\mathbf{b}_I^\alpha}_{I \in \mathcal{N}_\Lambda} \right] \tag{7}$$

where $\mathbf{u}_I$ is the nodal displacement vector associated with the continuous part of the finite element solution, $\mathbf{a}_I$ is the enriched nodal DOF vector associated with the Heaviside enrichment function, and $\mathbf{b}_I^\alpha$ is the enriched nodal DOF vector associated with the asymptotic crack-tip functions. In Eq. (7) $\mathcal{N}$ is the set of all nodes in the mesh, $\mathcal{N}_\Gamma$ is the set of nodes whose shape function is cut by the crack, and $\mathcal{N}_\Lambda$ is the set of nodes whose shape functions are cut by the crack tip. A visual representation of the nodes which have enriched degrees-of-freedom in XFEM is shown in Fig. 1.
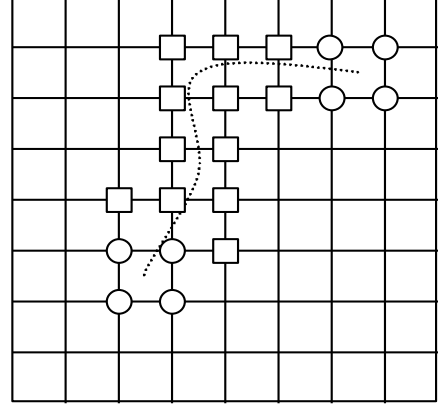
Using the Bubnov-Galerkin method to build the system of equations by using the approximation given in Eq. (7), we are able to derive a system of discrete linear equations is derived that will allow the solution of the nodal DOFs in our system of equations. The system of linear equations can be written in the form which is commonly associated with the finite element method as

Figure 1. Heaviside (squares) and crack tip (circles) enriched nodes for the crack shown.

$$[\mathrm{K}]\{\mathrm{q}\} = \{\mathrm{f}\} \tag{8}$$

where $\{q\} = \{u_I \quad a_I \quad b_I^1 \quad b_I^2 \quad b_I^3 \quad b_I^4\}^T$ is the vector of unknowns at the nodes, $[K]$ is the stiffness matrix given by

$$\mathrm{K}_{IJ} = \begin{bmatrix} \mathrm{K}_{IJ}^{uu} & \mathrm{K}_{IJ}^{ua} & \mathrm{K}_{IJ}^{ub} \\ \mathrm{K}_{IJ}^{au} & \mathrm{K}_{IJ}^{aa} & \mathrm{K}_{IJ}^{ab} \\ \mathrm{K}_{IJ}^{bu} & \mathrm{K}_{IJ}^{ba} & \mathrm{K}_{IJ}^{bb} \end{bmatrix} \tag{9}$$

$$\mathrm{K}_{IJ}^{\alpha\beta} = \int_\Omega \left(\mathrm{B}_I^\alpha \right)^{\mathrm{T}} \mathrm{C} \mathrm{B}_J^\beta \, d\Omega \quad (\alpha, \beta = u, a, b) \tag{10}$$

and $\{f\}$ is the external force vector defined as

$$\mathrm{f}_I = \left\{ \mathrm{f}_I^u, \mathrm{f}_I^a, \mathrm{f}_{I1}^b, \mathrm{f}_{I2}^b, \mathrm{f}_{I3}^b, \mathrm{f}_{I4}^b \right\} \tag{11}$$

$$f_I^u = \int_\Gamma N_I \bar{\mathrm{t}} d\Gamma + \int_\Omega N_I \mathrm{b} d\Omega \tag{12}$$

$$f_I^a = \int_\Gamma N_I H \bar{\mathrm{t}} d\Gamma + \int_\Omega N_I H \mathrm{b} d\Omega \tag{13}$$

$$f_{Ij}^b = \int_\Gamma N_I \Phi_j \bar{\mathrm{t}} d\Gamma + \int_\Omega N_I \Phi_j \mathrm{b} d\Omega \quad (j = 1-4). \tag{14}$$

In Eq. (10) C is the constitutive matrix for an isotropic linear elastic material, and B_I^u, B_I^a and B_{Ij}^b are the matrix of shape function derivatives in two-dimensions given by

$$B_I^u = \begin{bmatrix} N_{I,x} & 0 \\ 0 & N_{I,y} \\ N_{I,y} & N_{I,x} \end{bmatrix} \tag{15}$$

$$B_I^a = \begin{bmatrix} (N_I H)_{,x} & 0 \\ 0 & (N_I H)_{,y} \\ (N_I H)_{,y} & (N_I H)_{,x} \end{bmatrix} \tag{16}$$

$$B_I^b = \begin{bmatrix} B_{I1}^b & B_{I2}^b & B_{I3}^b & B_{I4}^b \end{bmatrix} \tag{17}$$

$$B_{Ij}^b = \begin{bmatrix} (N_I \Phi_j)_{,x} & 0 \\ 0 & (N_I \Phi_j)_{,y} \\ (N_I \Phi_j)_{,y} & (N_I \Phi_j)_{,x} \end{bmatrix}. \tag{18}$$

The system of equations from Eq. (8) can be solved to find the nodal displacements and nodal enrichment vectors. For detailed information on the integration of an enriched element, the reader is referred to Sukumar[9] for a discussion on element partitioning.

Sukumar[6] introduced a convenient way to represent the weak discontinuity created by a bi-material interface. The enrichment function for this discontinuity takes the form of

$$\upsilon(x) = |\zeta(x)| \tag{19}$$

where $\zeta(x)$ is the value of the level set function at a given point or is the shortest distance from any point in the domain to the discontinuity at the material interface. The shifted approximation takes the form given in Eq. (2). While this formulation is valid it requires an additional minimization process to reduce the relative error in the energy norm[6]. Another formulation to represent the material interface independent of the mesh is to use a formulation similar to the global-local finite element approximation[17].

III. Element-Based Enrichment for Material Interface

In this section, a new formulation for enrichment is proposed, which is similar to the global-local FEM. The global-local FEM was originally introduced by Mote[17] to incorporate global and local information about the finite element space into the finite element displacement field. The generalized global-local finite element approximation takes the form

$$u^h(x) = \sum_I N_I u_I + \upsilon(x) a_I \tag{20}$$

where $\upsilon(x)$ is the global enrichment function. The enrichment function $\upsilon(x)$ for the element-based enrichment is chosen such that

$$\upsilon(x) = \begin{cases} \upsilon_I(x) = 0 \\ \upsilon(\phi = 0) = 1 \end{cases} \tag{21}$$

where $\upsilon_I(x)$ is the value of $\upsilon(x)$ at node I, and ϕ is some general level set function tracking the material interface. Since the nodal value of the enrichment function are zero, the nodal displacement is given by Eq. (4). Furthermore, the function $\upsilon(x)$ is defined continuous across the interface, while its derivative is discontinuous.

The only difference in the element-based enrichment is to use Eq. (20) within an element. Thus, the enrichment function $\upsilon(x)$ is defined within an element and an additional DOF a_I for each spatial dimension is associated with the element. Since $\upsilon(x)$ has been defined to be one at the material interface the additional DOF a_I scale $\upsilon(x)$ such that the interpolation between elements across the domain is accurate. Only one additional spatial DOF will be needed to represent a bi-material element, unlike in the XFEM formulation where two additional spatial DOFs would be added at each node of a bi-material element. For integration the same element partitioning scheme used by Sukumar[9] is used in the element-based enrichment. The element-based enrichment is used to represent bi-material elements in this implementation.

IV. Level Set Method

The level set method is a versatile method for computing and analyzing the evolution of an interface Γ in two or three dimensions, which was introduced by Osher and Sethian[18]. The interface bounds an open region Ω. The velocity of the evolving interface can depend on position, time, interface geometry and the physics of the underlying problem. The level set function will be used for representing the material interface between the fiber and matrix as well as the geometry of a crack.

The level set function $\phi(x(t),t)$ is a continuous function, where $x(t)$ is a point in the domain Ω. The level set function has the following properties

$$
\begin{aligned}
\phi(x(t),t) < 0 \quad &\text{for } x \in \Omega \\
\phi(x(t),t) > 0 \quad &\text{for } x \notin \Omega \\
\phi(x(t),t) = 0 \quad &\text{for } x \in \Gamma
\end{aligned}
\tag{22}
$$

Therefore, the boundary of interest at any given time t can be located by finding $x(t)$ that satisfies the following equation:

$$
\phi(x(t),t) = 0 \tag{23}
$$

The boundary is commonly referred to as the zero level set of ϕ which can be abbreviated as ϕ_o. Equation (23) is commonly referred to as the level set equation. The typical approach to using the level set equation to propagate a moving front over time is to differentiate with respect to time which yields

$$
\frac{\partial \phi}{\partial t} + \frac{\partial x(t)}{\partial t} \cdot \frac{\partial \phi}{\partial x(t)} = 0 \tag{24}
$$

Equation (24) can be rewritten as

$$
\phi_{,t} + \vec{V} \cdot \nabla \phi = 0 \tag{25}
$$

where $\vec{V}$ is the velocity field. This partial differential equation can then be solved numerically by discretizing and using a finite difference approach to approximate the gradient of ϕ. The derivative of ϕ with respect to the time t can be approximated using the forward difference method as

$$
\frac{\phi^{n+1} - \phi^n}{\Delta t} + \vec{V}^n \cdot \nabla \phi^n = 0 \tag{26}
$$

which can be rewritten into a more convenient form for updating ϕ in two-dimensions as

$$\phi^{n+1} = \phi^n - \Delta t \left(u^n \phi^n_{,x} + v^n \phi^n_{,y} \right) \tag{27}$$

where u and v are the x and y components of the evolving interface velocity. The time step Δt is governed by the Courant-Friedrichs-Lewy (CFL) condition[19]. The CFL condition ensures that the approximation of the solution to the partial differential equation given in Eq. (24) is convergent. The limiting parameter for the time step in two-dimensions can be written as

$$\Delta t < \frac{\max\left(\Delta x, \Delta y\right)}{\max\left(u, v\right)} \tag{28}$$

where Δx and Δy represent the grid spacing in the x and y-directions.

For modeling a composite material, a fiber in a matrix will be considered. The level set function associated with a cylindrical fiber in the composite is denoted $\zeta(\boldsymbol{x})$ and calculated as

$$\zeta(\boldsymbol{x}) = \sqrt{\left(x_i - x_c\right)^2 + \left(y_i - y_c\right)^2} - r_c \tag{29}$$

where x_i and y_i are the coordinates of the ith node in the domain, x_c and y_c are the coordinates of the center of the fiber and r_c is the fiber radius.

The analytical form of the level set function as in Eq. (27) is limited for simple geometries. In addition, when the interface moves according to Eq. (23), the new interface will not have a simple analytical expression. Stolarska et al[4] introduced an extension of the level set method for modeling the evolution of a one-dimensional curve in a piecewise linear fashion with a particular focus on representing the evolution of a crack. Instead of having analytical expression of the level set function, a discrete value is assigned at each node of finite elements, and the location of zero level set is found using interpolation.

Sukumar[6] proposed additional enrichments via the level set method for the modeling of holes and inclusions. Two level set functions ϕ and ψ are needed to track the growth of an open curve in this case a crack: one for the crack path and the other for the crack tip. In this extension the crack path is represented as the zero level set of $\psi(x(t),t)$. The ψ level set is oriented such that its zero level set passes through the current crack tip and is oriented in the direction of the crack tip speed function. The zero level set of $\phi(x(t),t)$ is then given by the line intersecting the current crack tip and orthogonal to the zero level set of ψ.

For the ϕ and ψ level set functions, each grid point is assigned a distance from that point to the nearest point of that function's zero level set. The sign of the distance for the ψ level set function is positive on the side counter-clockwise from the direction of the crack tip speed function and negative on the clockwise side. The sign of the distance function for the ϕ function is positive on the side in the direction of crack growth and negative on the opposite side. The crack is defined to be the locations where the following conditions are true

$$\begin{aligned} \phi\left(x(t),t\right) &\leq 0 \\ \psi\left(x(t),t\right) &= 0 \end{aligned} \tag{30}$$

V.   Crack Growth Model

The amount of crack growth depends up on the chosen crack growth law and type of problem being solved. Paris crack growth law[2,4,10,20], has been used repeatedly to determine the amount of incremental crack growth. The maximum circumferential stress criterion is used to evolve the crack[8] in which the crack will propagate in the direction where $\sigma_{\theta\theta}$ is a maximum. The angle of crack growth[21] is given by

$$\theta_c = 2\arctan\frac{1}{4}\left(\frac{K_I}{K_{II}} - sign\left(K_{II}\right)\sqrt{\left(\frac{K_I}{K_{II}}\right)^2 + 8} \right) \tag{31}$$

American Institute of Aeronautics and Astronautics

where K_I and K_{II} are the mixed-mode stress intensity factors.

Thus, the direction of crack growth is a function of mixed-mode stress intensity factors. The domain forms of the interaction integrals[22,23] are used to calculate the mixed-mode stress intensity factors. For a general mixed-mode situation the relationship between the J-integral and the stress intensity factors can be given as

$$J = \frac{K_I^2}{E_{eff}} + \frac{K_{II}^2}{E_{eff}} \tag{32}$$

where E_{eff} is defined by a state of plane stress or plane strain as

$$E_{eff} = \begin{cases} E, & \text{plane stress} \\ \dfrac{E}{1-v^2}, & \text{plane strain} \end{cases} \tag{33}$$

where E is Young's modulus and v is Poisson's ratio. In order to calculate the mixed-mode stress intensity factors, an auxiliary stress state is superimposed onto the stress and displacement fields from the XFEM analysis. The auxiliary stress and displacement equations are chosen to be those derived by Westergaard[24] and Williams[25] which are given in the Appendix. The XFEM solutions are denoted with superscript (1) as $\sigma_{ij}^{(1)}$, $\varepsilon_{ij}^{(1)}$ and $u_i^{(1)}$, while that from the auxiliary state as $\sigma_{ij}^{(2)}$, $\varepsilon_{ij}^{(2)}$ and $u_i^{(2)}$.

Recall that the J-integral[26] takes the form of

$$J_i = \int_\Gamma \left[W n_i - \sigma_{jk} n_j \frac{\partial u_k}{\partial x_i} \right] d\Gamma \tag{34}$$

where W is the strain energy density and i denotes the crack tip opening direction, which is assumed to correspond to the global x-direction, denoted x_1. Equation (34) can be rewritten into a more convenient form as

$$J_1 = \int_\Gamma \left[W \delta_{1j} - \sigma_{ij} \frac{\partial u_i}{\partial x_1} \right] n_j d\Gamma . \tag{35}$$

The two stress states can be superimposed into Eq. (35) such that

$$J_1^{(1+2)} = \int_\Gamma \left[\frac{1}{2} \left(\sigma_{ij}^{(1)} + \sigma_{ij}^{(2)} \right) \left(\varepsilon_{ij}^{(1)} + \varepsilon_{ij}^{(2)} \right) \delta_{1j} - \left(\sigma_{ij}^{(1)} + \sigma_{ij}^{(2)} \right) \frac{\partial \left(u_i^{(1)} + u_i^{(2)} \right)}{\partial x_1} \right] n_j d\Gamma . \tag{36}$$

The J-integrals for pure state 1 and auxiliary state 2 can be separated from Eq. (36), which leaves an interaction term such that

$$J_1^{(1+2)} = J_1^{(1)} + J_1^{(2)} + I^{(1,2)} \tag{37}$$

where $I^{(1,2)}$ is the interaction term and is given by

$$I^{(1,2)} = \int_\Gamma \left[W^{(1,2)} \delta_{1j} - \sigma_{ij}^{(1)} \frac{\partial u_i^{(2)}}{\partial x_1} - \sigma_{ij}^{(2)} \frac{\partial u_i^{(1)}}{\partial x_1} \right] n_j d\Gamma \tag{38}$$

where $W^{(1,2)}$ is the interaction strain energy density

$$W^{(1,2)} = \sigma_{ij}^{(1)} \varepsilon_{ij}^{(2)} = \sigma_{ij}^{(2)} \varepsilon_{ij}^{(1)} \,. \tag{39}$$

Since we are superimposing two cracked configurations onto one another we can also write Eq. (32) as

$$J_1^{(1+2)} = \frac{\left(K_I^{(1)} + K_I^{(2)}\right)^2}{E_{eff}} + \frac{\left(K_{II}^{(1)} + K_{II}^{(2)}\right)^2}{E_{eff}} \,. \tag{40}$$

Expanding and rearranging terms from Eq. (40) yields

$$J_1^{(1+2)} = J_1^{(1)} + J_1^{(2)} + \frac{2\left(K_I^{(1)} K_I^{(2)} + K_{II}^{(1)} K_{II}^{(2)}\right)}{E_{eff}} \,. \tag{41}$$

Setting Eq. (37) and Eq. (41) equal leads to the relationship

$$I^{(1,2)} = \frac{2\left(K_I^{(1)} K_I^{(2)} + K_{II}^{(1)} K_{II}^{(2)}\right)}{E_{eff}} \,. \tag{42}$$

The stress intensity factors for the current state can be found by separating the two modes of fracture. By selecting $K_I^{(2)} = 1$ and $K_{II}^{(2)} = 0$, we are able to solve for $K_I^{(1)}$ such that

$$K_I^{(1)} = \frac{2 I^{(1,\text{Mode I})}}{E_{eff}} \,. \tag{43}$$

A similar procedure can also be followed such that $K_{II}^{(1)}$ is given by

$$K_{II}^{(1)} = \frac{2 I^{(1,\text{Mode II})}}{E_{eff}} \,. \tag{44}$$

The contour defining $I^{(1,2)}$ is converted to an area integral by using a smoothing function q. This function takes a value of 1 on the innermost contour and a value of 0 on the outermost contour. At any point in A, the linear shape functions are used to interpolate the value of q. The divergence theorem can be used to give the following equation for the domain form of the interaction integral.

$$I^{(1,2)} = \int_A \left[\sigma_{ij}^{(1)} \frac{\partial u_i^2}{\partial x_1} - \sigma_{ij}^{(2)} \frac{\partial u_i^1}{\partial x_1} - W^{(1,2)} \delta_{1j} \right] \frac{\partial q}{\partial x_j} \, \mathrm{d}A \tag{45}$$

VI.   Results

A. Crack in Finite Plate Under Tension

To verify that the implementation of XFEM and the domain form of the J-integral has been completed correctly, a test case is chosen and the results are compared to published values. The reference values were taken from Stress Intensity Factors Handbook Vol. 2[27]. A finite rectangular plate with a horizontal edge crack was loaded in tension as shown in Fig. 2. The theoretical Mode I stress intensity factor K_I for this configuration is given as

$$K_I = F(\lambda)\sigma\sqrt{\pi a} \tag{46}$$

where σ is the applied nominal stress, a is the crack length and $F(\lambda)$ is a factor associated with the finite effect of the plate[28] given by

$$F(\lambda) = 1.12 - 0.231\lambda + 10.55\lambda^2 - 21.72\lambda^3 + 30.39\lambda^4 \tag{47}$$

and λ is the ratio between the crack length and the width of the plate given as

$$\lambda = \frac{a}{W} \tag{48}$$

where W is the width of the plate. To compare the calculated and theoretical values, the stress intensity factors are normalized such that

$$K_{i,norm} = \frac{K_{i,calc}}{K_{i,theo}}. \tag{49}$$

An example of the geometry and finite element mesh are shown in Fig. 2. The results for a variety of λ are presented in Table **1**. It is noted that the XFEM with enrichment functions accurately calculate stress intensity factors.
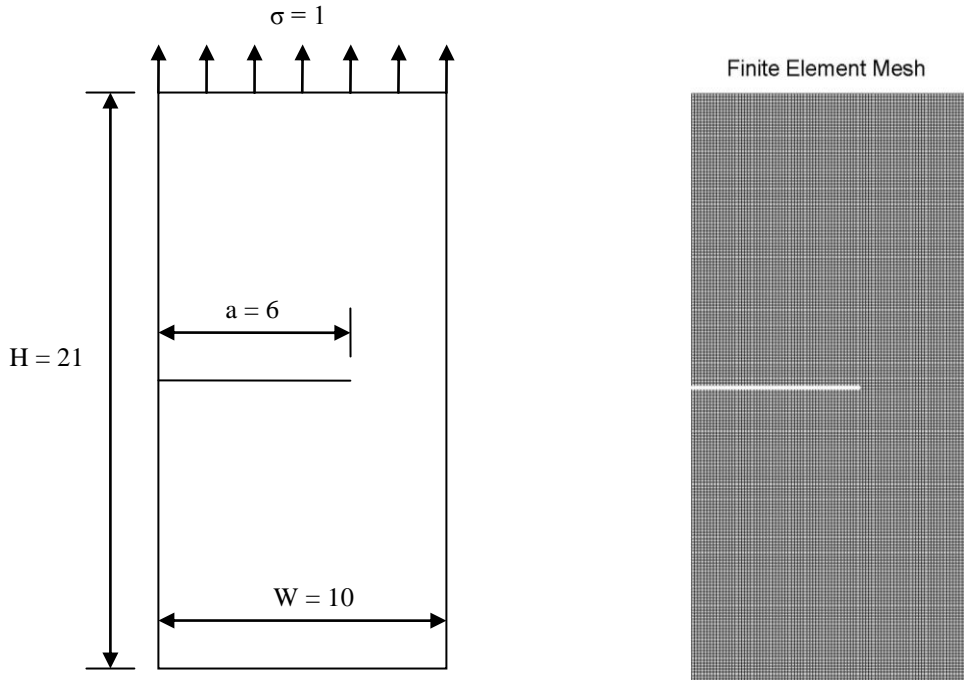

Figure 2. The geometry and finite element mesh of the cracked body for a crack length of 0.6.

Table 1. Comparison of calculated and theoretical Mode I stress intensity factors for a finite plate.

a	W	λ	F(λ)	$K_{I,theo}$	$K_{I,calc}$	$K_{I,norm}$	Percent Error
0.1	10	0.1	1.1837	2.0981	2.1187	1.0098	0.98
0.2	10	0.2	1.3707	3.4357	3.4406	1.0014	0.14
0.3	10	0.3	1.6599	5.0959	5.1052	1.0018	0.18
0.4	10	0.4	2.1035	7.4567	7.4780	1.0029	0.29
0.5	10	0.5	2.8264	11.2018	11.1420	0.9947	0.53
0.6	10	0.6	4.0264	17.4812	17.3434	0.9921	0.79

B. Element-based Enrichment for a Bi-material Bar

A simple one-dimension bar was modeled using the element-based enrichment function presented in Eq. (20) to ensure that the approximation was valid before extending the approximation into two-dimensions. The general case shown in Fig. 3 was considered. To simplify the presentation, a single element is used to model the entire bar.
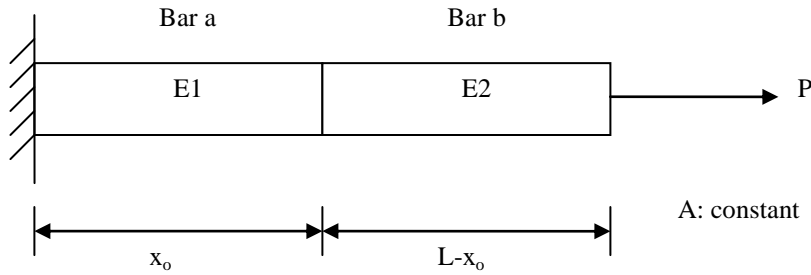

Figure 3. The bi-material bar to be modeled using the element-based enrichment.

In the element-based enrichment, a single function is required for each element. The enrichment function $\upsilon(x)$ takes the form

$$\upsilon(x) = \begin{cases} x/x_o & 0 \le x \le x_o \\ (L-x)/(L-x_o) & x_o \le x \le L \end{cases}. \tag{50}$$

Note that the above enrichment function is piece-wise linear.

The global vector of degrees-of-freedom is defined by $\{\mathbf{q}\} = \{u_1 \quad u_2 \quad a\}$ where a is the degree-of-freedom associated with the enrichment function. From the Bubnov-Galerkin method, the stiffness and force matrix for this case can be represented as

$$K_e = \int_0^{x_o} \{B\} EA \{B\}^T \, dx + \int_{x_o}^L \{B\} EA \{B\}^T \, dx = K_e^1 + K_e^2 \tag{51}$$

$$K_e^1 = \frac{EA}{L^2} \begin{bmatrix} x_o & -x_o & L \\ -x_o & x_o & -L \\ L & -L & L^2/x_o \end{bmatrix} \tag{52}$$

$$K_e^2 = \frac{EA}{L^2} \begin{bmatrix} L-x_o & x_o-L & L \\ x_o-L & L-x_o & -L \\ L & -L & L^2/(L-x_o) \end{bmatrix} \qquad (53)$$

$$\{F\} = \{F_1, F_2, 0\}^T . \qquad (54)$$

The bar element should be able to accurately predict the displacement of a bar through interpolating between nodes using two nodal displacement values and the enriched DOF a. Once the two nodal values have been found, interpolation between the nodes can be found using Eq. (20). The element-based bar element should be able to handle the case where the materials of bars a and b shown in Fig. 3 are identical. First the single material case is considered. Next two cases are considered where the discontinuity is at L/2 and L/4. In all cases the theoretical values are compared to the element-based enrichment solution. For all examples other than the homogeneous bar, E1 = 1, E2 = 10, A = 1, L = 1, and P = 1 were used. The displacement plots for the single material case is shown in Fig. 4 and the bi-material cases are shown in Fig. 5.
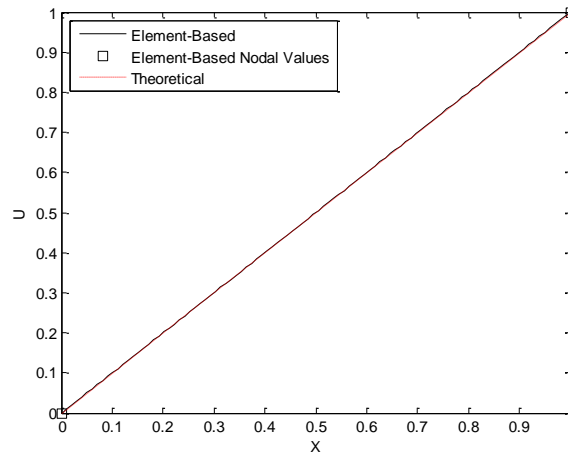

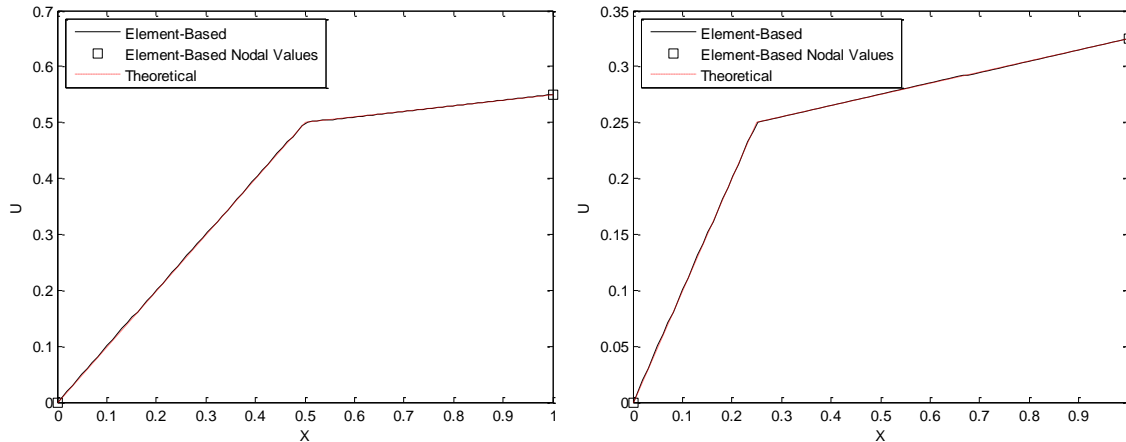**Figure 4. Comparison of global-local approximation and theoretical values for a single material.**

Figure 5. Comparison of global-local approximation and theoretical values for a middle (right) and offset (left) discontinuity.

A closed-form solution of the enriched degree of freedom a for this case takes the form

$$a = \frac{PL}{A}\left(\frac{1}{E_1} - \frac{1}{E_2}\right)\left(\frac{x_o}{L}\right)\left(1 - \frac{x_o}{L}\right). \tag{55}$$

The same bi-material bar problem can be solved using a single element in XFEM. If the enrichment from Eq. (1) is used the interpolation between nodes is not piecewise linear without the additional constraint $a_1 = a_2$. If the shifted enrichment function from Eq. (3) is used the piecewise linear behavior is recovered, but additional degrees of freedom are needed when compared to the element-based formulation.

C. Element-based Enrichment for a Circular Inclusion

The global-local approximation was extended into two-dimensions. In this case the enrichment function $\upsilon(x)$ is created using the constant strain triangle approach where $\upsilon(x)$ satisfies Eq. (21). A plate with a circular inclusion in plane strain was modeled using the element-based enrichment in two-dimensions. The finite element mesh and stress plots for a bi-material case where the plate has E = 50 GPa and the inclusion has E = 70 GPa and equivalent Poisson's ratio of 0.33 are shown in Fig. 6. These results match very well with that from commercial finite element software. Note that some of the apparent stress irregularities around the location of the material interface are introduced by the plotting routine and may not be representative of the calculated stresses at all points.
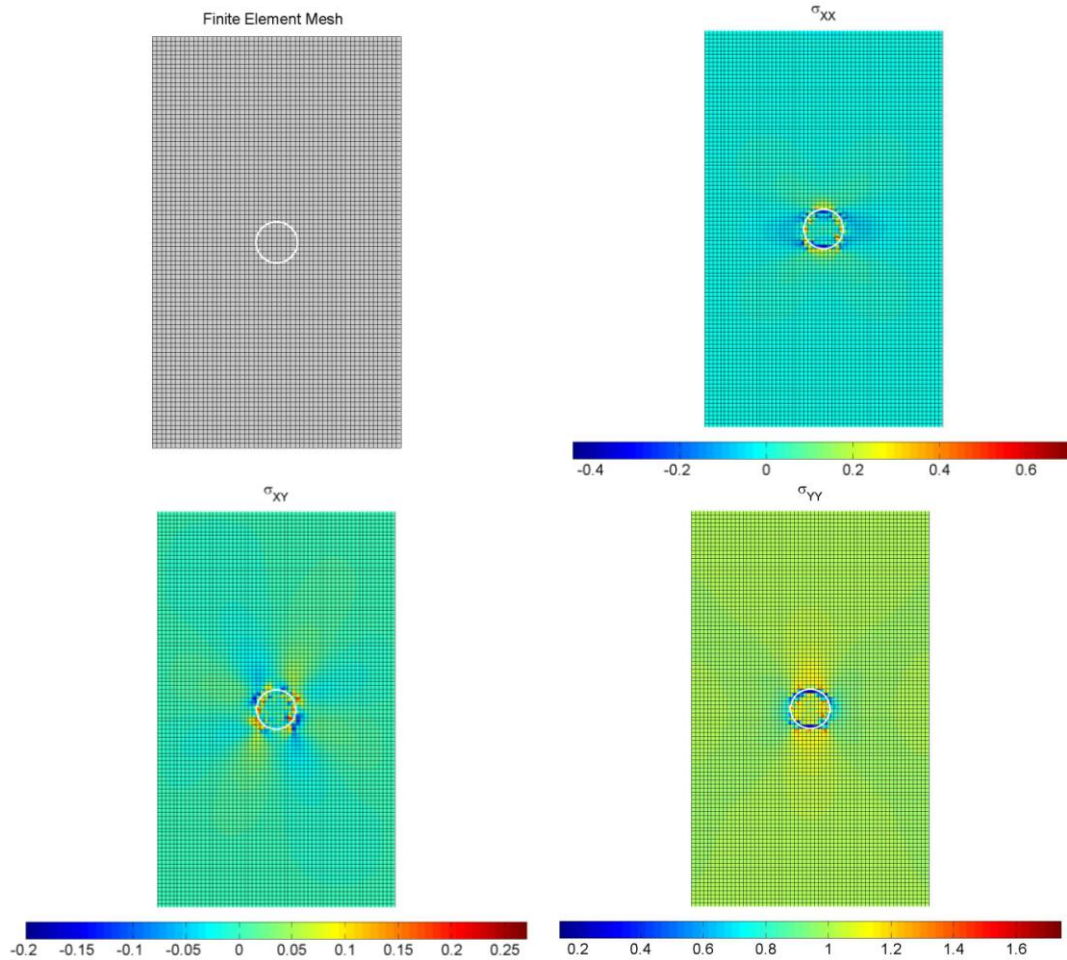

Figure 6. The finite element mesh and stress plots for a circular inclusion in a plate with hole location superimposed on all plots.

VII. Conclusion

The modeling of crack growth is a challenge in the conventional finite element method. The difficulties associated with remeshing as a crack grows in FEM can be eliminated by the use of XFEM. XFEM uses enrichment functions and additional degrees of freedom to include information about strong and weak discontinuities independent of the mesh. Formulations for crack interfaces in the XFEM were presented as well as an element-based enrichment formulation for modeling bi-material interfaces. A convenient method to calculate the mixed-mode stress intensity factors was discussed as well as an algorithm for crack growth.

It was shown that the combined XFEM and element-based enrichment can accurately calculate the Mode I stress intensity factor for a pure Mode I crack. It has also been shown that the implementation can accurately handle domains cut by a crack. In the future the implementation will be expanded to include crack growth criteria as a crack approaches an interface with a specific goal of accurately predicting whether the crack will penetrate or deflect around a fiber reinforcement causing debonding to occur in the composite material.

Appendix

The auxiliary stresses derived by Westergaard[24] and Williams[25] are

$$\sigma_{11} = \frac{1}{\sqrt{2\pi r}}\left\{K_I \cos\frac{\theta}{2}\left[1-\sin\frac{\theta}{2}\sin\frac{3\theta}{2}\right]-K_{II}\sin\frac{\theta}{2}\left[2+\cos\frac{\theta}{2}\cos\frac{3\theta}{2}\right]\right\} \tag{A1}$$

$$\sigma_{22} = \frac{1}{\sqrt{2\pi r}}\left\{K_I \cos\frac{\theta}{2}\left[1+\sin\frac{\theta}{2}\sin\frac{3\theta}{2}\right]+K_{II}\sin\frac{\theta}{2}\cos\frac{\theta}{2}\cos\frac{3\theta}{2}\right\} \tag{A2}$$

$$\sigma_{33} = v\left(\sigma_{11}+\sigma_{22}\right) \tag{A3}$$

$$\sigma_{23} = \frac{1}{\sqrt{2\pi r}}K_{III}\cos\frac{\theta}{2} \tag{A4}$$

$$\sigma_{31} = \frac{-1}{\sqrt{2\pi r}}\sin\frac{\theta}{2} \tag{A5}$$

$$\sigma_{12} = \frac{1}{\sqrt{2\pi r}}\left\{K_I \sin\frac{\theta}{2}\cos\frac{\theta}{2}\cos\frac{3\theta}{2}+K_{II}\cos\frac{\theta}{2}\left[1-\sin\frac{\theta}{2}\sin\frac{3\theta}{2}\right]\right\} \tag{A6}$$

and the auxiliary displacements are

$$u_1 = \frac{1}{2\mu}\sqrt{\frac{r}{2\pi}}\left\{K_I \cos\frac{\theta}{2}\left(\kappa-\cos\theta\right)+K_{II}\sin\frac{\theta}{2}\left(\kappa+2+\cos\theta\right)\right\} \tag{A7}$$

$$u_2 = \frac{1}{2\mu}\sqrt{\frac{r}{2\pi}}\left\{K_I \sin\frac{\theta}{2}\left(\kappa-\sin\theta\right)+K_{II}\cos\frac{\theta}{2}\left(\kappa-2+\cos\theta\right)\right\} \tag{A8}$$

$$u_3 = \frac{2}{\mu}\sqrt{\frac{r}{2\pi}}K_{III}\sin\frac{\theta}{2} \tag{A9}$$

where μ is the shear modulus and κ is the Kosolov constant.

References

[1]Belytschko, T., Black, T., "Elastic crack growth in finite elements with minimal remeshing." *International Journal for Numerical Methods in Engineering,* Vol. 45, 1999, pp. 601-620.

[2]Belytschko, T., Moës, N., Usui, S., Parimi, C., "Arbitrary discontinuities in finite elements." *International Journal for Numerical Methods in Engineering,* Vol. 50, 2001, pp. 993-1013.

[3]Moës, N., Dolbow, J., Belytschko, T., "A finite element method for crack growth without remeshing." *International Journal for Numerical Methods in Engineering,* Vol. 46, 1999, pp. 131-150.

[4]Stolarska, M., Chopp, D., Moës, N., Belytschko, T., "Modelling crack growth by level sets in the extended finite element method." *International Journal for Numerical Methods in Engineering,* Vol. 51, 2001, pp. 943-960.

[5]Sukumar, N., Chopp, D., Moran, B., "Extended finite element method and fast marching method for three-dimensional fatigue crack propagation." *Engineering Fracture Mechanics,* Vol. 70, 2003, pp. 29-48.

[6]Sukumar, N., Chopp, D., Moës, N., Belytschko, T., "Modeling holes and inclusions by level sets in the extended finite-element method." *Computer Methods in Applied Mechanics and Engineering,* Vol. 190, 2001, pp. 6183-6200.

[7]Daux, C., N, M., Dolbow, J., Sukumar, N., Belytschko, T., "Arbitrary branched and intersecting cracks with the extended finite element method." *International Journal for Numerical Methods in Engineering,* Vol. 48, 2000, pp. 1741-1760.

[8]Moës, N., Gravouil, A., Belytschko, T., "Non-planar 3D crack growth by the extended finite element and level sets - Part I: Mechanical model." *International Journal for Numerical Methods in Engineering,* Vol. 53, 2002, pp. 2549-2568.

[9]Sukumar, N., Prévost, J., "Modeling quasi-static crack growth with the extended finite element method Part I: Computer implementation." *International Journal of Solids and Structures,* Vol. 40, 2003, pp. 7513-7537.

[10]Gravouil, A., Moës, N., Belytschko, T., "Non-planar 3D crack growth by the extended finite element and level sets - Part II: Level set update." *International Journal for Numerical Methods in Engineering,* Vol. 53, 2002, pp. 2569-2586.

[11]Sukumar, N., Chopp, D., Béchet, E., Moës, N., "Three-dimensional non-planar crack growth by a coupled extended finite element and fast marching method." *International Journal for Numerical Methods in Engineering,* Vol. 00, 2007, pp. 1-39.

[12]Sukumar, N., Huang, Z., Prévost, J., Suo, Z., "Partition of unity enrichment for bimaterial interface cracks." *International Journal for Numerical Methods in Engineering,* Vol. 59, 2004, pp. 1075-1102.

[13]Unger, J., Eckardt, S., Könke, C., "Modelling of cohesive crack growth in concrete structures with the extended finite element method." *Computer Methods in Applied Mechanics and Engineering,* Vol. 196, 2007, pp. 4087-4100.

[14]Zi, G., Belytschko, T., "New crack-tip elements for XFEM and applications to cohesive cracks." *International Journal for Numerical Methods in Engineering,* Vol. 57, 2003, pp. 2221-2240.

[15]Hettich, T., Hund, A., Ramm, E., "Modeling failure in composites by X-FEM and level sets within a multiscale framework." *Computer Methods in Applied Mechanics and Engineering,* Vol. 197, 2008, pp. 414-424.

[16]Hettich, T., Ramm, E., "Interface material failure modeled by the extended finite-element method and level sets." *Computer Methods in Applied Mechanics and Engineering,* Vol. 195, 2006, pp. 4753-4767.

[17]Mote, C., "Global-local finite element." *International Journal for Numerical Methods in Engineering,* Vol. 3, 1971, pp. 565-574.

[18]Osher, S., Sethian, J., "Fronts propagating with curvature dependent speed: Algorithms based on Hamilton-Jacobi formulations." *Journal of Computational Physics,* Vol. 79, 1988, pp. 12-49.

[19]Courant, R., Friedrichs, K., Lewy, H., "On the partial difference equations of mathematical physics." *Mathematische Annalen,* Vol. 100, 1928, pp. 32-74.

[20]Guidault, P., Allix, O., Champaney, L., Cornuault, C., "A multiscale extended finite element method for crack propagation." *Computer Methods in Applied Mechanics and Engineering,* Vol., 2007, pp.

[21]Erdogan, F., Shih, G., "On the crack extension in plates under plane loading and transverse shear." *Journal of Basic Engineering,* Vol. 85, 1963, pp. 519-527.

[22]Shih, C., Asaro, R., "Elastic-plastic analysis of cracks on bimaterial interfaces: part I - small scale yielding." *Journal of Applied Mechanics,* Vol. 55, 1988, pp. 299-316.

[23]Yau, J., Wang, S., Corten, H., "A mixed-mode crack analysis of isotropic solids using conservation laws of elasticity." *Journal of Applied Mechanics,* Vol. 47, 1980, pp. 335-341.

[24]Westergaard, I., "Bearing pressures and cracks." *Journal of Applied Mechanics, Transactions ASME,* Vol. 61, 1939, pp. A49-A53.

[25]Williams, M., "On the stress distribution at the base of a stationary crack, ." *Journal of Applied Mechanics,* Vol. 24, 1957, pp. 109-114.

[26]Rice, J., "A path integral and the approximate analysis of strain concentration by notches and cracks." *Journal of Applied Mechanics,* Vol. 35, 1968, pp. 379-386.

[27]Mukamai, Y. (ed.), *Stress Intensity Factors Handbook*, Pergamon Press, 1987.

[28]Brown, W., Srawley, J., "Plain strain crack toughness testing of high-strength metallic materials." *ASME STP 410,* Vol., 1966, pp. 12.